Sensors

Ultrasensitive and Selective Copper(II) Detection: Introducing a Bioinspired and Robust Sensor

Lena K. Müller[+],[b] Ivana Duznovic[+],[c] Daniel Tietze,[a] Wadim Weber,[d] Mubarak Ali,[e] Viktor Stein,[d] Wolfgang Ensinger,[c] and Alesia A. Tietze*[a, b]

Abstract: A nanopore-based Cu^{II}-sensing system is reported that allows for an ultrasensitive and selective detection of Cu^{II} with the possibility for a broad range of applications, for example in medical diagnostics. A fluorescent ATCUN-like peptide 5/6-FAM-Dap-β-Ala-His is employed to selectively bind Cu^{II} ions in the presence of Ni^{II} and Zn^{II} and was crafted into ion track-etched nanopores. Upon Cu^{II} binding the fluorescence of the peptide sensor is quenched, permitting the detection of Cu^{II} in solution. The ion transport characteristics of peptide-modified nanopore are shown to be extremely sensitive and selective towards Cu^{II} allowing to sense femtomolar Cu^{II} concentrations in human urine mimics. Washing with EDTA fully restores the Cu^{II}-binding properties of the sensor, enabling multiple repetitive measurements. The robustness of the system clearly has the potential to be further developed into an easy-to-use, lab-on-chip Cu^{II}-sensing device, which will be of great importance for bedside diagnosis and monitor of Cu^{II} levels in patients with copper-dysfunctional homeostasis.

Copper is an essential trace element that is inevitable in biological systems and can be found in many enzymes such as amine oxidases and ferroxidases but is also required for infant growth, the iron metabolism and brain development in human organisms.[1] It is also widely used in agricultural systems, and therefore belongs to a major metal pollutant in our environment.[2] There are also diseases linked to a toxic copper concentration and/or dysregulated copper metabolism in humans such as Wilson's disease, Menke's and Alzheimer's disease (AD).[3]

During the last two decades studies have been performed in order to confirm the involvement of copper in β-amyloid plaques procession.[4] During a meta-analysis performed by Squitti et al. the concentration of free copper in the serum of AD patients is determined to be higher compared to that of healthy patients.[5] These results are generated by studying the fraction of copper that is not bound to ceruloplasmin (non-CP Cu) and include all studies from 1996 until early 2013. Recent studies of Squitti et al. show the extraordinary medical interest of "free copper" detection in urine as an eligible marker for patients in early stages of Alzheimer's disease.[6] Thus, determination of non-bound Cu^{II} in urine and serum can be used as a basis for a screening method for the early diagnosis and/or monitoring of diseases linked to abnormal copper concentrations, for example AD or Wilson's disease.[3] However, fast and reliable quantification of non-CP Cu in body fluids is still a major challenge (e.g. see Ref. [7] and references cited therein) urging for the need of fast screening methods and sensors for selective and sensitive detection of copper(II) ions. As a recent example, Squitti et al. designed a fluorescent method to detect non-CP Cu^{II} ions.[5] Nonetheless, this method is performed in a two-step experimental set-up comprising a size exclusion solid-phase extraction separating non-CP Cu from protein-bound copper followed by a direct fluorescent method and thus being rather time consuming. It is a well-known fact that peptides and proteins can display extraordinary and ultra-sensitive key–lock behavior towards targets. Natural copper-bind-

[a] *Dr. D. Tietze, Prof. Dr. A. A. Tietze*
University of Gothenburg
Department of Chemistry and Molecular Biology
Wallenberg Centre for Molecular and Translational Medicine
Kemigården 4, 412 96 Göteborg (Sweden)
E-mail: alesia.a.tietze@gu.se

[b] *Dr. L. K. Müller,[+] Prof. Dr. A. A. Tietze*
Technische Universität Darmstadt
Clemens-Schöpf Institute of Organic Chemistry and Biochemistry
Alarich-Weiss Str. 4, 64287 Darmstadt (Germany)

[c] *I. Duznovic,[+] Prof. Dr. W. Ensinger*
Technische Universität Darmstadt
Fachbereich Material- und Geowissenschaften
Fachgebiet Materialanalytik
Alarich-Weiss-Str. 2, 64287 Darmstadt (Germany)

[d] *W. Weber, Prof. Dr. V. Stein*
Technische Universität Darmstadt
Department of Biology
Schnittsphanstrasse 12, 64287 Darmstadt (Germany)

[e] *Dr. M. Ali*
GSI Helmholtzzentrum für Schwerionenforschung
Materialforschung
Planckstraße 1, 64291 Darmstadt (Germany)

[+] *These authors contributed equally to this work.*

Supporting information and the ORCID identification number(s) for the author(s) of this article can be found under: https://doi.org/10.1002/chem.202001160.

ing proteins and peptides are albumins (bovine serum albumin (BSA), human serum albumin (HSA), rabbit serum albumin (RSA)), neuromedin C and K, human sperm protamine P2a and histatins.[8] Based on the natural occurring Cu^{II} binding motifs, Imperiali et al. reported a set of polypeptide motifs for the design of selective Cu^{II} ion chemosensors.[9] In their work, they expanded the Cu^{II} binding motif by incorporating unnatural amino acids into the widely used Cu^{II} complexing tripeptide (Gly-Gly-His), leaving only His at its mandatory position. Further, they incorporated a linker unit and an amine-containing sidechain for the attachment of a fluorescence group.[9] The combination of this peptide-based Cu^{II} binding motif with a fluorescent probe, which fluorescent properties are modulated (turned "on" or "off") upon Cu^{II} binding are among the most promising chemosensors.[3,10] Based on the natural occurring Cu^{II} binding motif, Papp et al. covalently attached the amino terminal Cu^{II}- and Ni^{II}-binding motif (ATCUN motif) (Gly-Gly-His) to gold-plated track-etched polycarbonate membranes resulting in a nanopore-based Cu^{II} sensor.[11] This demonstrates an example of a robust hybrid system with a limit of detection (LOD) in the submicromolar range and a good linearity between 10^{-3}–10^{-6} M.[11] Another copper-sensing systems that can be evaluated by naked eye detection with a detection limit of 0.5 μM using a "turn-on" fluorescence strategy was reported by Situ et al., however, with the disadvantage that the detection method involves several reaction steps.[12] Further, naked eye sensor systems were constructed by Ding et al. developing a colorimetric detection of copper using sensor strips at a detection limit of 5 nM.[13] Aiming for surface-crafted sensors Zheng et al. integrated a fluorescent Cu-sensing moiety into a PEG hydrogel resulting into a reversible fluorescence quenching of 73.6% upon Cu^{II}-binding making the sensor reusable. However, the decrease of fluorescence takes about 18 hours, leaving room for improvement.[14] Due to the above-mentioned disadvantages of the known copper sensing methods and the need for highly sensitive and selective detection methods for Cu^{II} ions it is an objective of current work to provide a sensor allowing a fast and easy-to-handle, but highly selective and ultra-sensitive qualitative and quantitative detection of Cu^{II} ions in solutions.

Thus, the following study reports a robust nanopore-based Cu^{II} sensing system which allows for an ultrasensitive and selective detection of Cu^{II}, which will allow for the development of stand-alone Cu^{II}-sensing device. A fluorescent ATCUN-like peptide 5/6-FAM-Dap-β-Ala-His was crafted into track-etched nanopores to selectively bind Cu^{II} ions in the presence of Ni^{II} and Zn^{II} (Figure 1). The concentration of Cu^{II} in an analyte solution is determined by current–voltage (*I–V*) characteristics of the nanopore, and fluorescence microscopy by detection of concentration-dependent fluorescence quenching.

Inspired by the ATCUN-like metal binding motif we designed a peptide-like sequence possessing a fluorophore, using 5,6-carboxyfluorescein (5/6-FAM) as a response group. A polyethylene glycol (PEG) moiety, attached to the C-terminus of the functional peptide was used to ensure a spatial separation of the peptide from the solid support (Figure 1) resulting in an overall sequence of 5/6-FAM-Dap-β-Ala-His-PEG4 (referred to as peptide **1** hereafter, Figure 2). Thereby, the metal-binding motif is composed of the three residues Dap-β-Ala-His (Figure 2), remaining only one natural amino acid at C-terminal position, which was reported to be mandatory for Cu-binding.[9]

We additionally generated a non-fluorescent version of peptide **1** which lacks the 5/6-FAM moiety (referred to as peptide **2** hereafter) (Figure 2, Figure S1 and S2). Before the ATCUN-like peptides **1** and **2** are crafted to the nanopores their binding and selectivity properties towards Cu^{II}, Ni^{II} and Zn^{II}, which are naturally present in human fluids at low concentrations[15] and in environmental samples as trace elements, are studied in detail in solution. Therefore, metal binding is studied through metal titration experiments utilizing fluorescence and UV/Vis spectroscopy. First of all, the addition of increasing concentrations of Zn^{II} sulfate to peptide **1** and **2** has no impact on the fluorescence or UV/Vis spectra (Figure S3), indicating that no peptide-Zn^{II} complex is formed.[9] In contrast, the characteristic *d–d* transition bands at 537 nm and 438 nm are observed for peptide **2** with Cu^{II} or Ni^{II}, which unveils the formation of square planar Cu^{II} and Ni^{II} complexes with peptide **2** (Figure 3a).[8,16] Furthermore, UV/Vis-based Cu^{II} and Ni^{II} titration experiments (Figure 3b, Figures S8–S11) with peptide **2** indicate

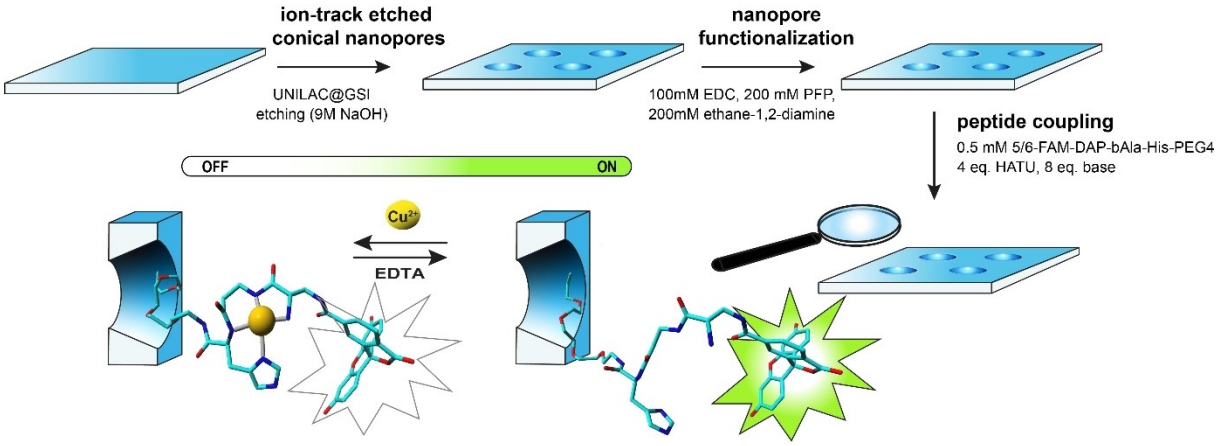

Figure 1. Cu-sensor design and composition based on ion-track etched polyethylene terephthalate (PET) membranes.

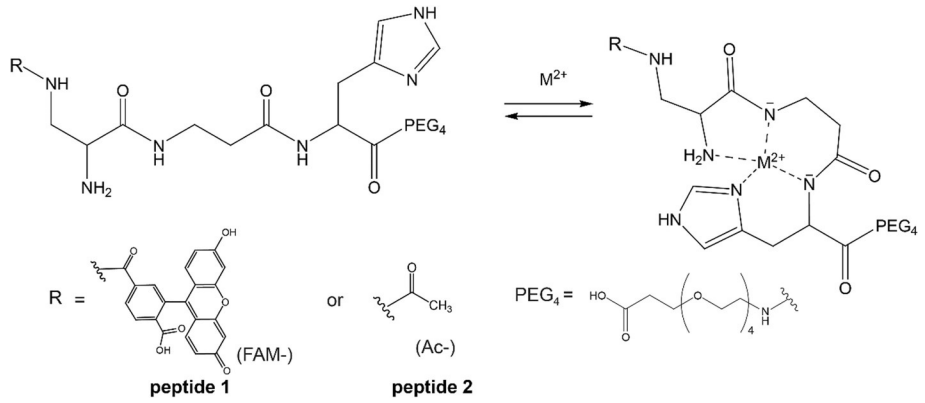

Figure 2. Representation of the ATCUN-like Cu^{II} and Ni^{II} binding motif. Structure of the Dap-β-Ala-His motif and proposed metal coordination (FAM-Dap-β-Ala-His–peptide **1**, Ac-Dap-β-Ala-His–peptide **2**, FAM −5/6 carboxyfluorescein, Ac–acetylated N-terminus).

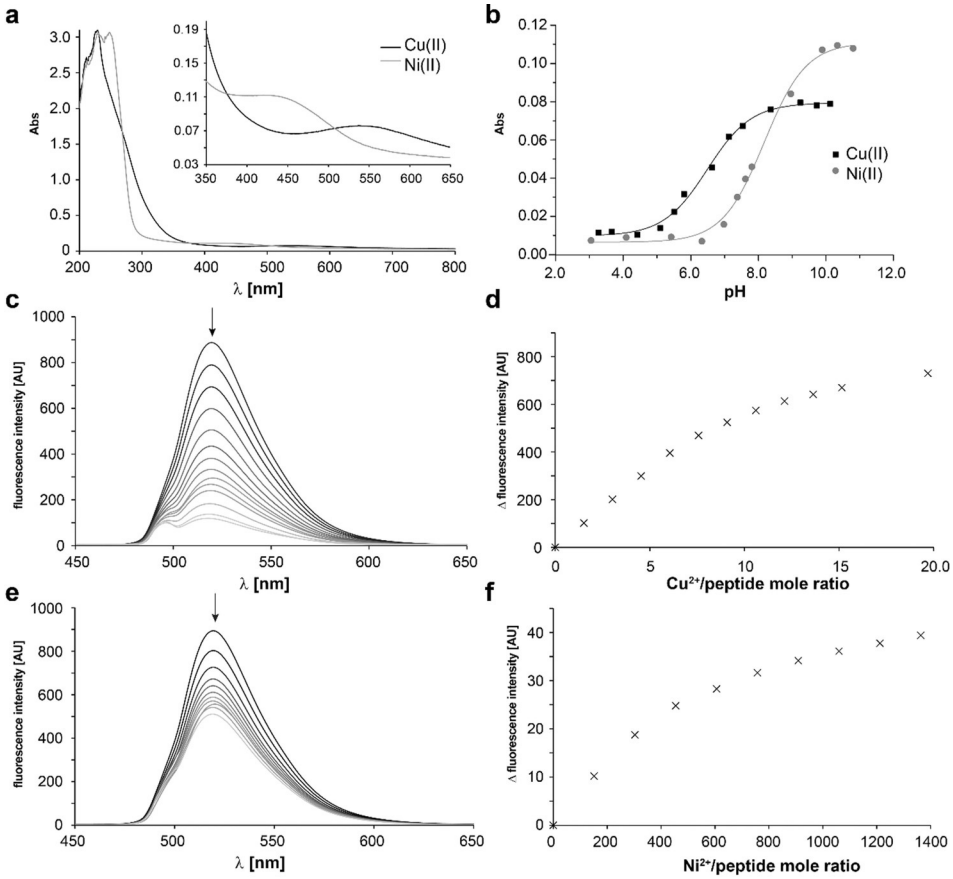

Figure 3. Spectroscopic characterization of metal complex formation. a) UV/Vis spectra of Cu^{II} (black) and Ni^{II} (grey) complex with peptide **2** (1 mM, 100 mM Tris buffer, 25 °C) at pH 8 (Cu^{II}) and pH 10.5 (Ni^{II}). b) UV/Vis spectroscopic determination of pH dependency of Cu^{II} (black) and Ni^{II} (grey) complex formation with peptide **2** (1 mM, water, 25 °C) followed at 537 nm (Cu^{II}) and 438 nm (Ni^{II}). c–f) fluorescence spectroscopic characterization of peptide **1** with $CuSO_4$ and $NiSO_4$ (excitation at λ_{Ex} 494 nm, emission at λ_{Em} 518, 25 °C). c) decrease of fluorescence intensity of peptide **1** (1 μM, 100 mM MES buffer pH 6.5) upon addition of $CuSO_4$ (0–25 μM, in water). d) change of fluorescence intensity as a function of the molar ratio of Cu^{II} to peptide **1**. e) decrease of fluorescence intensity of peptide **1** (1 μM, 100 mM MES buffer[20] pH 6.5) upon addition of $NiSO_4$ (0–1.3 mM, in water). **f** change of fluorescence intensity as a function of the molar ratio of Ni^{II} to peptide **1**.

a 1:1 metal–peptide complex with Cu^{II} at pH 6.5 and with Ni^{II} at pH 10.5, whereas peptide **2** most likely distally coordinates an additional Cu^{II} ion at pH 8.0 through some of the remaining free amide or amine nitrogen atoms. ESI mass spectrometry (MS) (Figure S4–S7) and the experimental isotope patterns derived thereof, further support the formation of a 1:1 complex of peptide **1** and **2** with either Cu^{II} or Ni^{II} ions and are in a good agreement with simulated isotopic patterns and literature data for these kind of systems (Figures S4–S7).[9,16,17] Interestingly, peptide to metal complex formation for both peptides

1 and **2** is observed to be highly pH-dependent. With respect to our UV/Vis data, the complexation of Cu^{II} by peptide **2** occurs in a pH range from 5 to 8, while Ni^{II} complexation falls in the pH range between 6.5 to 10 (Figure 3b) concluding, that Cu^{II} ions can be selectively detected in the presence of Ni^{II} at a pH of 6.5 (Figure 3b, Figures S10, S11). As we realized that metal complex formation with peptide **1** is accompanied with a significant quench of its fluorescence, Cu^{II} and Ni^{II} titration experiments were studied in detail by fluorescence spectroscopy (Figure 3c–f, Figures S12, S13). This also circumvent tedious analysis of the UV/Vis data of the fluorescent peptide due to the strong overlap of the absorption band of the fluorescent moiety with the ligand-to-metal transition at 438 and 537 nm, respectively. Therefore, fluorescence at the emission maximum of 518 nm was first studied at a pH, which was determined to be optimal for the complex formation with Cu^{II} or Ni^{II} by UV/Vis spectroscopy. When one equivalent of Cu^{II} is added to peptide **1** at pH 8.0 fluorescence intensity quickly decreases by 89% (11% remaining intensity) (Figure S12). Similarly, upon addition of one equivalent of Ni^{II} to peptide **1** at pH 10.5 a remaining fluorescence of 29% is observed (Figure S13). In contrast, Cu^{II} addition to peptide **1** at pH 6.5, at which a selective Cu^{II} detection can be achieved results in a decrease of fluorescence intensity by 88% (12% remaining fluorescence intensity), when 20 equivalents of Cu^{II} are added (Figure 3c,d). In comparison a much larger excess of Ni^{II} (>1300 equivalents) is necessary at this pH in order to observe a decrease of fluorescence intensity by approx. 43% (57% remaining fluorescence intensity, Figure 3e,f). In turn, almost no change of the fluorescence intensity is observable when only 20 equivalents of Ni^{II} are added, which corresponds to the amount of Cu^{II} yielding an almost complete fluorescence quench. According to our UV/Vis data of peptide **2**, this observation can be explained by the insufficient formation of the peptide **1**–Ni^{II} complex at pH 6.5. Instead, UV/Vis spectra of peptide **2** show, that upon Ni^{II} addition a low intensity absorption band is formed at 394 nm indicating the formation of non-specific octahedral peptide **2**–Ni^{II} complex (Figure S11).[8] Additionally, we further determined the binding constants (K_b) at pH 8.0 (Cu^{II}) and pH 10.5 (Ni^{II}) as well as at pH of 6.5 (Table S1).

For Cu^{II} binding to peptide **2** the constant is derived from our UV/Vis data using the Benesi–Hildebrand method and appeared to be 1.0×10^{6} M (3.8×10^{6} M at pH 6.5) (Figure S14). Under the same conditions but utilizing the fluorescence data the Cu^{II} binding constant of peptide **1** is derived from the Stern–Volmer plot yielding a somewhat higher value of 2.1×10^{9} M (6.27×10^{6} M at pH 6.5) (Figure S15, Equations S1–S3), which agree well with literature values of analogue peptides.[17a,b,18] Although the Ni^{II} binding constants at pH 10.5 of peptide **1** (6.15×10^{11} M) and **2** (2.5×10^{7} M) are higher compared to Cu^{II}, they are much lower at pH 6.5 (1.80×10^{3} M peptide **1**, 5.80×10^{2} M peptide **2**) demonstrating again the outstanding selectivity towards Cu^{II} ions (Table S1). Also, we determined the quenching rate constant (K_q) for peptide **1** by studying the fluorescence quenching behavior. The value of quenching rate constant towards copper is 2.75×10^{13} l×M and the quenching behavior can be described by static quenching with the formation of a non-fluorescent complex in the ground state (Equation S2), thus allowing to monitor Cu^{II} binding by fluorescence microscopy. In summary, by choosing the optimal pH the DAP-βAla-His motif is selective towards copper(II) in presence of nickel(II) and zinc(II) ions, which has not been reported for any other ATCUN-like motifs before.[19] Interestingly, the limit of detection (LOD) of Cu^{II} ions in solution with peptide **1** using fluorescence spectroscopy is 13.5 nM (Figure S16) being of great importance giving any possible applications, that is, for detection of trace amounts of Cu^{II} in food/water control/environmental samples or as a diagnostic tool for diseases, which are connected to a copper dyshomeostasis, such as Wilson or even Alzheimer's diseases.[6] Having determined the selectivity and sensitivity of peptides **1** and **2** towards Cu^{II}, Ni^{II} and Zn^{II} ions in solution and observing no differences in binding behavior of both peptides we crafted our peptide **1**, containing the fluorophore, to an ion-track etched nanopore (Figure 1).

By crafting peptide **1** into nanopores, we are aiming to achieve a sensor for example, environmental or medical applications. For that purpose, polymer membranes containing conical nanopores (10^4 pores/cm^2) were fabricated via asymmetric chemical etching of the latent track of energetic heavy ions resulting in nanopores with tip opening of 30 ± 5 nm and base opening of 500 ± 10 nm in diameter (Figure 1).[21] As a result of heavy ion irradiation and subsequent chemical etching, carboxylic acid groups are generated on the pore surface, which are then employed for the covalent attachment of ethylenediamine providing a primary amine for consequent coupling of peptide **1** at its C-terminal PEG-linker (Figure 2). To monitor the chemical functionalization process on the nanopore surface, we carried out *I–V* measurements after each surface modification steps. After successful peptide immobilization we studied the Cu^{II} sensing capabilities of the nanopore exposing it to an electrolyte solution containing different concentration of $CuCl_2$ (Figure 4a). Our *I–V* measurements show that before Cu^{II} complexation the modified nanopore is rectifying, not allowing anions to pass being in the so-called "off" state (Figure S17). The complexation of Cu^{II} by peptide **1** at pH 6.5 crafted to a nanopore generates positive charges on the pore surface, which concomitantly changes the ion transport behavior of the nanopore. The pore becomes anion selective as evidenced from the successive increase in positive current by increasing Cu^{II} concentration starting in the femtomolar range (Figure 4a,b). After a nanomolar Cu^{II} concentration is reached, no further increase of the positive current is observed, suggesting that the peptide is entirely folded and complexed with Cu^{II}. In contrast, even micromolar Cu^{II} ion concentration (≤10 μM) could not alter the transport characteristics of the as-prepared pore.

This clearly demonstrates that the presence of peptide-Cu^{II} complexes on the pore walls and surface switches the pore transport behavior from nonconducting "off" state to conducting "on" state. The copper cation acts as a chemical trigger to control the electrostatic behavior of the modified pore due to host–guest recognition process taking place in this confined environment (Figure 4a). Finally, our data show that the pep-

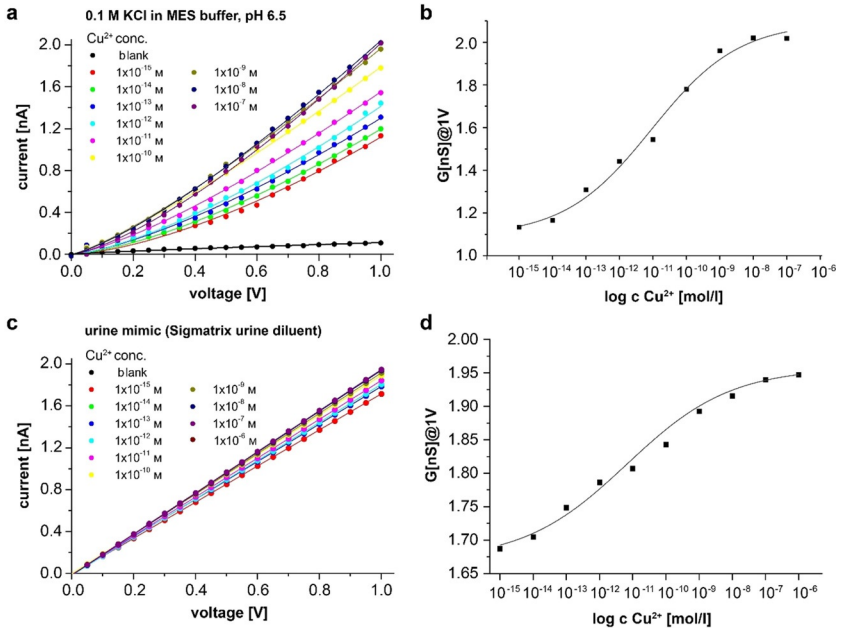

Figure 4. Cu-sensor *I–V* characteristics of peptide **1** in nanopore in MES buffer (a,b) and urine mimic (c,d). a,c) *I–V* titration response of peptide **1** nanopore on different concentration of $CuSO_4$. b,d) Conductance of the peptide-modified pore at different Cu^{II} concentrations in the electrolyte solution.

tide-modified nanopore is able to recognize Cu^{II} ions even at very low concentrations, and this recognition process can be transduced in an electronic signal originating from the transport behavior of the nanopore (Figure 4b). Similar to these *I–V* measurements in 0.1 M KCl solution in MES puffer, the peptide-modified nanopore system can even selectively bind Cu^{II} in Sigmatrix urine diluent, which mimics human urine (Figure 4c). A linear response to the Cu^{II} concentrations in the urine mimic was achieved in the range of 1×10^{-14} to 1×10^{-7} mol l^{-1} (Figure 4d). Moreover, our *I–V* measurements suggest a fully reversible Cu^{II} binding to the nanopore as Cu^{II} can be extracted from the peptide by washing with EDTA (Figure S17b, Figure 5a,b). Aside from metal detection through *I–V* measurements the fluorescent properties of the peptide-modified nanopore system can also be utilized according to our metal binding experiments with peptide **2** in solution utilizing confocal laser scanning microscopy (CLSM). Indeed, after successful binding of the peptide on the PET material the modified nanopore is clearly visible in the CLSM image (Figure 5) and appeared as green spots on the PET surface when excited by a laser at 488 nm (Figure 5b).

To investigate the behavior towards copper(II), nickel(II) and zinc(II) ions, we set up titration experiments similar to our experiments in solution and determined the modified PET foil's re-usability as well as the shelf-life (Figure 5c,d, Figure S18). Fluorescence quenching experiments at pH 6.5 indicate a decrease in fluorescence intensity of the nanopore-bound fluorescent peptide after addition of Cu^{II} (0–100 μM, in MES pH 6.50) with a linear dependency up to 60 μM (Figure 5c) whereas no changes of the fluorescence intensity is observed when similar Ni^{II} or Zn^{II} concentrations were used (Figure S18). However, a millimolar $NiSO_4$ solution is needed in order to induce some fluorescence quenching (Figure S18a,c), while the addition of high concentrations of $ZnSO_4$ (up to 100 mM) does not affect the fluorescence intensity (Figure S18b,d). Furthermore, once Cu^{II} is bound to the peptide-modified nanopore, it can be removed by washing the PET foil with EDTA (Figure 5d) and the foil can be re-used for Cu^{II} detection. So far, we were able to re-use the foil seven times for Cu^{II} sensing without losing its Cu^{II} sensing capabilities or detection performance even though the modified PET foil was stored for more than six months.

We have found that the fluorescent and non-fluorescent versions of an ATCUN-like peptide which is based on the metal binding motif Dap-β-Ala-His can be employed to specifically bind Cu^{II} ions in the presence of Ni^{II} and Zn^{II}.

As the Cu^{II} and Ni^{II} complex formation of the ATCUN-like peptide is pH dependent Cu^{II} selectivity can be controlled via the pH of the solution. Fluorescence quenching occurred when the peptide-metal complex is formed achieving a selective and highly sensitive Cu^{II} detection with an LOD of 13.5 nM. *I–V* measurements and CLCM data show, that Cu^{II} selectivity and metal-binding induced fluorescence quenching properties are preserved when the peptide is bound to the nanopore. The *I–V* characteristics of the peptide-nanopore system are highly sensitive towards Cu^{II} allowing for the detection of femtomolar Cu^{II} concentrations in buffer but also in human urine mimics. Moreover, Cu^{II}-complex formation inside the nanopore can also be tracked by the subsequent loss in fluorescence intensity, thus, allowing for a selective Cu^{II} detection in the range of 1 to 100 μM. Lastly, Cu^{II} ions can be removed from the nanopore system by washing with EDTA which fully restores the Cu^{II}-binding properties, enabling repetitive measurements up to six times.

Moreover, this concept is significantly more robust and sensitive than other current Cu^{II} sensor systems, such as systems

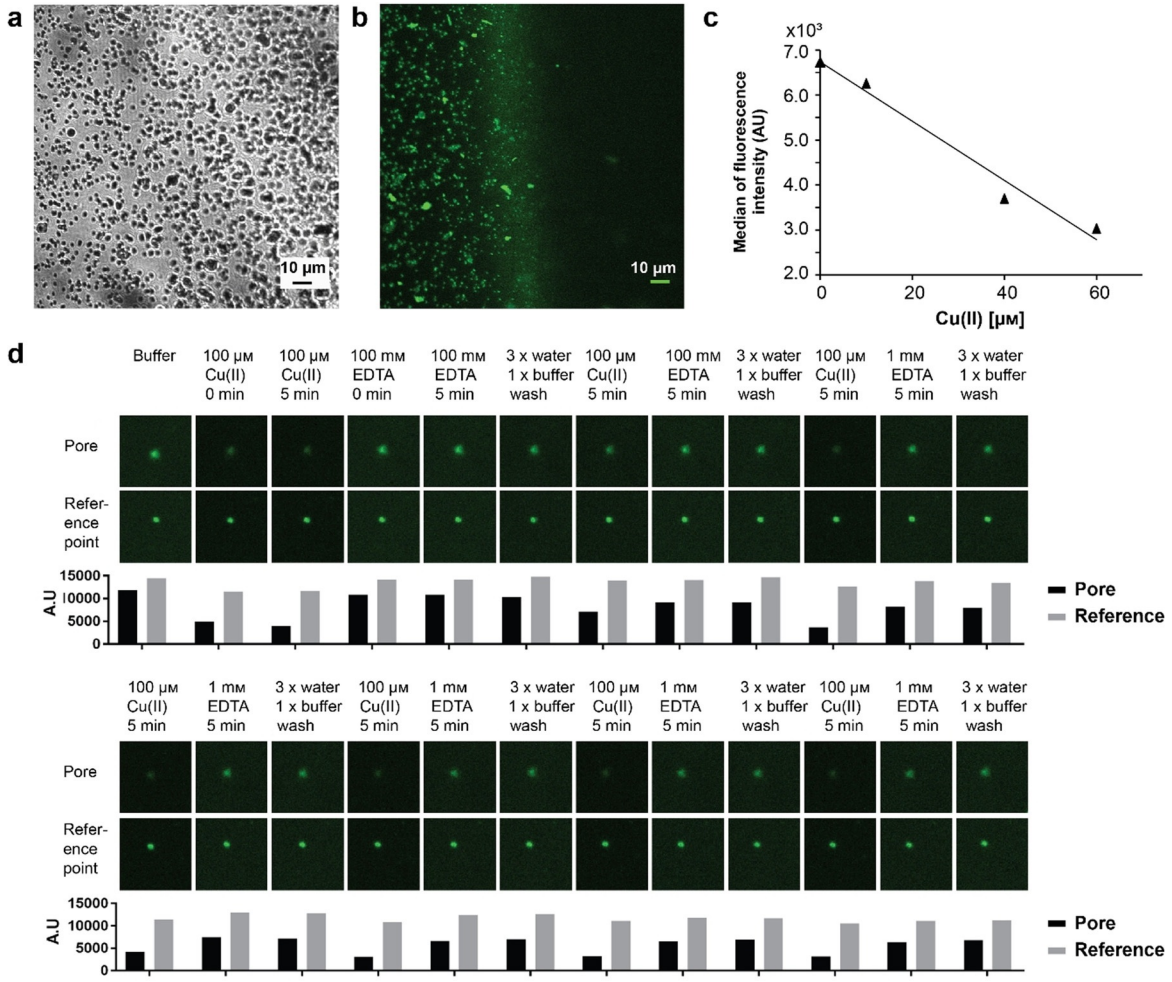

Figure 5. Confocal laser scanning microscopy (CLSM) images of fluorescently labelled peptide **1** coupled to nanopores of a PET foil. a) reflected light and b) fluorescence emission image. Area without fluorescence in (b) representing pores that were not etched and thus not modified. c) decrease in fluorescence intensity (median) after addition of $CuSO_4$ (0–60 µM, in MES buffer). d) CLSM of "on-off" characteristics showing re-usability after regenerating with 1 mM EDTA and washing with water and MES buffer pH 6.5 (fluorescence excitation at λ_{Ex} 488 nm, emission detected at λ_{Em} 515–530 nm).

employing β-cyclodextrin functionalized α-hemolysin pores in planar lipid bilayers[22] or PU membrane-based nanopores using Cu-binding nanoparticles, whose translocation speed through the nanopore allows for Cu^{II} detection after 24 h of incubation.[23]

The robustness of the system clearly has the potential to be further developed into an easy-to-use, lab-on-chip Cu^{II}-sensing device, which is currently under development in our lab. Such device, of which the current nanopore system will be the key component, will be of great importance for on-bed diagnosis and monitor of Cu^{II} levels in patients with copper dyshomeostasis, such as in Wilson and Alzheimer's disease.[6,7,24]

Consequently, this nanopore system enables a selective, sensitive and fast Cu^{II} detection by either *I–V* measurements or fluorescence quenching opening up numerous possible applications.

Acknowledgements

Financial support for this project by the Liebig Fellowship of the Fonds der Chemischen Industrie (A.A.T), LOEWE project iNAPO funded by the Ministry of Higher education, Research and the Arts (HMWK) of the Hessen state (L.K.M., I.D., W.W., V.S., W.E., A.A.T) and the Knut and Alice Wallenberg Foundation are gratefully acknowledged (A.A.T). We thank Prof. C. Trautmann and Dr. Maria E. Toimil Molares from GSI Darmstadt for providing polymer foils.

Conflict of interest

The authors declare no conflict of interest.

Keywords: ATCUN · copper · fluorescence · nanopores · sensors

[1] a) B. E. Kim, T. Nevitt, D. J. Thiele, *Nat. Chem. Biol.* **2008**, *4*, 176–185; b) P. G. Georgopoulos, A. Roy, M. J. Yonone-Lioy, R. E. Opiekun, P. J. Lioy, *J. Toxicol. Environ. Health Part B* **2001**, *4*, 341–394.
[2] F. Pizarro, M. Olivares, V. Gidi, M. Araya, *Rev. Environ. Health* **1999**, *14*, 231–238.
[3] D. Wu, A. C. Sedgwick, T. Gunnlaugsson, E. U. Akkaya, J. Yoon, T. D. James, *Chem. Soc. Rev.* **2017**, *46*, 7105–7123.
[4] D. L. Sparks, B. G. Schreurs, *Proc. Natl. Acad. Sci. USA* **2003**, *100*, 11065–11069.
[5] R. Squitti, I. Simonelli, M. Ventriglia, M. Siotto, P. Pasqualetti, A. Rembach, J. Doecke, A. I. Bush, *J. Alzheimer's Dis.* **2014**, *38*, 809–822.
[6] R. Squitti, R. Ghidoni, I. Simonelli, I. D. Ivanova, N. A. Colabufo, M. Zuin, L. Benussi, G. Binetti, E. Cassetta, M. Rongioletti, M. Siotto, *J. Trace Elem. Med. Biol.* **2018**, *45*, 181–188.
[7] a) P. J. Gow, R. A. Smallwood, P. W. Angus, A. L. Smith, A. J. Wall, R. B. Sewell, *Gut* **2000**, *46*, 415–419; b) F. Woimant, N. Djebrani-Oussedik, A. Poujois, *Ann. Transl. Med.* **2019**, *7*, S70.
[8] C. Harford, B. Sarkar, *Acc. Chem. Res.* **1997**, *30*, 123–130.
[9] A. Torrado, G. K. Walkup, B. Imperiali, *J. Am. Chem. Soc.* **1998**, *120*, 609–610.
[10] S. Liu, Y.-M. Wang, J. Han, *J. Photochem. Photobiol. C* **2017**, *32*, 78–103.
[11] S. Papp, G. Jagerszki, R. E. Gyurcsanyi, *Angew. Chem. Int. Ed.* **2018**, *57*, 4752–4755; *Angew. Chem.* **2018**, *130*, 4842–4845.
[12] B. Situ, J. Zhao, W. Lv, J. Liu, H. Li, B. Li, Z. Chai, N. Cao, L. Zheng, *Sens. Actuators B* **2017**, *240*, 560–565.
[13] B. Ding, Y. Si, X. Wang, J. Yu, L. Feng, G. Sun, *J. Mater. Chem.* **2011**, *21*, 13345–13353.
[14] Y. Zheng, K. M. Gattás-Asfura, C. Li, F. M. Andreopoulos, S. M. Pham, R. M. Leblanc, *J. Phys. Chem. B* **2003**, *107*, 483–488.
[15] J. Versieck, *Crit. Rev. Clin. Lab. Sci.* **1985**, *22*, 97–184.
[16] K. P. Neupane, A. R. Aldous, J. A. Kritzer, *J. Inorg. Biochem.* **2014**, *139*, 65–76.
[17] a) Y. Zhang, S. Akilesh, D. E. Wilcox, *Inorg. Chem.* **2000**, *39*, 3057–3064; b) K. Kulprachakarn, Y. L. Chen, X. Kong, M. C. Arno, R. C. Hider, S. Srichairatanakool, S. S. Bansal, *J. Biol. Inorg. Chem.* **2016**, *21*, 329–338; c) K. P. Neupane, A. R. Aldous, J. A. Kritzer, *Inorg. Chem.* **2013**, *52*, 2729–2735.
[18] M. Sokolowska, A. Krezel, M. Dyba, Z. Szewczuk, W. Bal, *Eur. J. Biochem.* **2002**, *269*, 1323–1331.
[19] a) Y. Zheng, K. M. Gattas-Asfura, V. Konka, R. M. Leblanc, *Chem. Commun.* **2002**, 2350–2351; b) Y. Xiang, A. Tong, P. Jin, Y. Ju, *Org. Lett.* **2006**, *8*, 2863–2866.
[20] Q. Yu, A. Kandegedara, Y. Xu, D. B. Rorabacher, *Anal. Biochem.* **1997**, *253*, 50–56.
[21] P. Y. Apel, Y. E. Korchev, Z. Siwy, R. Spohr, M. Yoshida, *Nucl. Instrum. Methods Phys. Res. Sect. B* **2001**, *184*, 337–346.
[22] a) Y. Guo, F. Jian, X. Kang, *RSC Adv.* **2017**, *7*, 15315–15320; b) L. Wang, F. Yao, X. F. Kang, *Anal. Chem.* **2017**, *89*, 7958–7965; c) G. Wang, L. Wang, Y. Han, S. Zhou, X. Guan, *Biosens. Bioelectron.* **2014**, *53*, 453–458.
[23] a) L. J. Mayne, S. D. Christie, M. Platt, *Nanoscale* **2016**, *8*, 19139–19147; b) I. Heaton, M. Platt, *Anal. Chem.* **2019**, *91*, 11291–11296.
[24] a) S. Bagheri, R. Squitti, T. Haertle, M. Siotto, A. A. Saboury, *Front. Aging Neurosci.* **2017**, *9*, 446; b) M. Loef, H. Walach, *Br. J. Nutr.* **2012**, *107*, 7–19.

Manuscript received: March 6, 2020
Accepted manuscript online: March 20, 2020
Version of record online: June 17, 2020